The 2014 World Congress on
Advances in Civil, Environmental, and Materials Research (ACEM14)
Busan, Korea, August 24-28, 2014

Nonlinear damage detection using higher statistical moments of structural responses

Ling Yu[*,1-2)] and Jun-Hua Zhu[2-3)]

[1)] *Department of Mechanics and Civil Engineering, Jinan University, Guangzhou 510632, China*
[2)] *MOE Key Lab of Disaster Forecast and Control in Engineering, Jinan University, Guangzhou 510632, China*
[3)] *The 5th Electronics Research Institute of the Ministry of Industry and Information Technology, Guangzhou 510610, China*

ABSTRACT

An integrated method is proposed for structural nonlinear damage detection based on time series analysis and the higher statistical moments of structural responses in this study. It combines the time series analysis, the higher statistical moments of AR model residual errors and the fuzzy c-means (FCM) clustering techniques. A few comprehensive damage indexes are developed in the arithmetic and geometric manner of the higher statistical moments, and are classified by using the FCM clustering method to achieve nonlinear damage detection. A series of the measured response data, downloaded from the web site of the Los Alamos National Laboratory (LANL) USA, from a three-story building structure considering the environmental variety as well as different nonlinear damage cases, are analyzed and used to assess the effectiveness and robustness of the new nonlinear damage detection method. Some valuable conclusions are made and related issues discussed as well.

1. INTRODUCTION

Structural damage detection (SDD) plays the most pivotal role in the process of structural health monitoring (SHM) (Gul and Catbas 2011). Currently, the vibration-based damage detection technique has been recognized and intensively studied as a promising tool for monitoring structural conditions and detecting structural damages (Doebling et al. 1998, Yan et al. 2001, Sohn et al. 2004, Carden and Fanning 2004, Zhou et al. 2013, Yu et al. 2013). SDD is arguably one of the most critical components of SHM. Identifying the presence of the damage might be considered as the first step to

* Corresponding author, Professor L. Yu, E-mail: lyu1997@163.com
[1)] Professor
[3)] Senior Engineer

take preventive actions and to start the process towards understanding the root causes of the problem (Gul and Catbas 2011). Most of these vibration-based damage detection methods can be classified into two groups: model based and feature based (Zhang 2007). For the latter, especially for those based on the time series statistical analysis in constructing time-series signature for direct damage diagnosis have gained considerable attention recently since their implementation for an automated SHM system is relatively more feasible compared to the model based methods (Lu and Gao 2005, Chen and Yu 2013, Yao and Pakzad 2014).

Most of the time series analysis based methodologies aim to fit time series models to the vibration data and then try to detect the damage by extracting damage features from these time series models. As one of key steps in the SHM, the ideal approach for features extraction is to choose features that are sensitive to damage, but are not sensitive to operational and environmental variations. However, such an approach is not always possible in real-world structures, and intelligent feature extraction procedures are usually required (Worden et al. 2007). Some of them directly compare the time series models whereas some of them use the residual errors when the new data is used with the previously created model. In a statistical manner, these methodologies usually make use of AR (Auto-Regressive) (Fugate et al. 2001, Gul and Catbas 2009, Zugasti et al. 2012, Yao and Pakzad 2014), ARX (Auto-Regressive models with eXogenous outputs) (Sohn and Farrar 2001, Lu and Gao 2005, Gul and Catbas 2011), ARMA (Auto-Regressive Moving Average) (Nair et al. 2006, Omenzetter and Brownjohn 2006, Carden and Brownjohn 2008) and ARMA/GARCH models (Chen and Yu 2013) to detect the damage of structures.

Fugate et al. (2001) fitted an AR model to the measured acceleration-time-histories from an undamaged structure, defined the residual errors quantifying the difference between the prediction from the AR model and the actual measured time history at each time interval as the damage-sensitive features, and employed X-bar and S control charts to monitor the mean and variance of the selected features for structural damage detection. Zugasti et al. (2012) presented the application of two damage detection methods to a laboratory tower. The second one was based on AR modeling of the signals involved. The results showed that two methods were able to correctly detect damage in the structure that was simulated by loosening some of the bolts in the joints, but the second method is more stable. As potentially competitive damage detection techniques, Yao and Pakzad (2012) proposed and studied two time series-based structural damage detection algorithms using statistical pattern recognition. One of them uses the Ljung-Box statistic of AR model residual sequence as damage index, the other uses the Cosh spectral distance of the estimated AR model spectrum. Compared with existing algorithms based on AR model residual variance and coefficients distance, the Ljung-Box statistic provides a more accurate account of the structural damage and Cosh spectral distance is less sensitive to changes in excitation sources. Subsequent applications to vibration data from simulation and lab experiments show that the Ljung-Box statistic is indeed a more sensitive feature than residual variance in most cases, while Cosh spectral distance tends to be more stable than Mahalanobis distance of coefficients. Further, Yao and Pakzad (2014) derived the sensitivity expressions of two damage features, namely the Mahalanobis distance of AR coefficients and the Cosh distance of AR spectra, with respect to both structural damage and measurement noise

level. The effectiveness of the proposed methods was illustrated in a numerical case study on a 10-DOF system, where their results were compared with those from direct simulation and theoretical calculation.

Sohn and Farrar (2001) proposed a two-step AR-ARX (auto-regressive and auto-regressive with eXogenous) model to predict the time series and subsequently used the standard deviation (STD) ratio of the residual error to indicate the damage. Lu and Gao (2005) developed a novel method to construct a novel auto-regressive time-series signature for the diagnosis of structural damage. The model stems from the linear dynamics and is formulated in the form of the ARX model involving only the (acceleration) response data. When the reference model is applied on the measured response of an unknown state, the STD of the residual error is used as a damage feature. Gul and Catbas (2011) extracted different damage features from ARX models created for the different clusters. Although the proposed methodology showed great success for the examples under investigation, the authors also acknowledged that the methodology should be verified with more laboratory experiments using different types of structures and the methodology should also be improved for damage detection with ambient vibration data.

Nair et al. (2006) used an ARMA model and used the first three AR components as the damage sensitive feature and they were able to identify and locate the damage. Omenzetter and Brownjohn (2006) used Auto-Regressive Integrated Moving Average (ARIMA) models to analyze the static strain data from a bridge during construction and when it was opened to service. Although the authors were able to detect structural changes with the methodology, they also acknowledged that the location and severity of the damage could not be identified. Carden and Brownjohn (2008) presented a statistical classification algorithm based on analysis of a structural response in the time domain. The time-series responses are fitted with ARMA models and the ARMA coefficients are fed to the classifier. The approach is demonstrated with experimental data from the IASC-ASCE benchmark four-storey frame structure, the Z24 bridge and the Malaysia-Singapore Second Link bridge. The classifier is found to be capable of identifying structural change in all cases and of forming distinct classes corresponding to different structural states in most cases. However, the approach may not be the most suitable SHM paradigm for structures with only ambient dynamic excitation.

However, all of studies mentioned above are based on linear AR, ARX and/or ARMA models and assumed the residual error obeys normal distribution. Unfortunately, the states with the nonlinearities show that an assumption of normality is not justified in the real world (Figueiredo et al., 2009). This assumption often increase misdiagnosis rate because the damage information main focused on the tails of distribution where slight deviations from the normal condition can be seen. These traditional linear time series analysis based methods cannot deal with nonlinear damages effectively, such as the fatigue cracks that open and close upon dynamic loading (Chen and Yu 2013). Apart from the mean and standard deviation of the time histories, Mattson and Pandit (2006) also used the higher-order moments of the residuals obtained from vector AR models to detect damage. They pointed out that the residual-based method is capable of identifying non-linear damage signatures that are too deeply buried in the system dynamics to be identified directly from the raw data, but found that only use of skewness and kurtosis as features for damage diagnosis is less reliable than the

variance (Carden and Brownjohn 2008). However, Figueiredo et al. (2009) concluded that the skewness and kurtosis show some differences in the damaged states when compared to the undamaged states conditions. They can be used as features to detect damage that results in a linear system subsequently exhibiting nonlinear dynamic response.

In this study, an integrated method is proposed for structural nonlinear damage detection based on time series analysis, the higher statistical moments of structural responses and the fuzzy c-means (FCM) clustering techniques. Six comprehensive damage indexes are developed in the arithmetic and geometric manner of the higher statistical moments, and are classified by using the FCM clustering method to achieve nonlinear damage detection. The background of theory of the integrated method is first presented in the section two. In order to assess the performance of the integrated nonlinear SDD method proposed in this study, some experimental data downloaded from the web site of the Los Alamos National Laboratory (LANL) USA on a three-story building structure are adopted to conduct experimental verification in the following section. The effectiveness and robustness of the new nonlinear SDD method are finally analyzed and concluded.

2. BACKGROUND OF THEORY

In this section, a procedure of the integrated method is presented based on time-series analysis. Based on linear system theory, *AR* time series models are used to describe the acceleration time histories and are used in the analysis of stationary time series processes. A stationary process is a stochastic process, one that obeys probabilistic laws, in which the mean, variance and higher order moments are time invariant.

2.1 Data standardization

Supposing $x_i \in R^{n\times 1}$ ($i=1,2...p$), denotes amplitudes of measured acceleration response data with p data sample at all n measurement points. In order to eliminate the effects caused by environmental and operational variations from the measured acceleration responses, the data standardization is necessary as follows

$$\hat{x}_i = \frac{x_i - \bar{x}}{\sigma} \tag{1}$$

$$\bar{x} = \frac{1}{p}\sum_{i=1}^{p} x_i \tag{2}$$

$$\sigma^2 = \frac{1}{p-1}\sum_{i=1}^{p}(x_i - \bar{x})^2 \tag{3}$$

Where, $\bar{x}$, σ^2 and $\hat{x}_i$ are the mean, variance and standardized version of time series signal x_i respectively.

2.2 Traditional damage-sensitive index

AR models attempt to account for the correlations of the current observation in time series with its predecessors. A univariate *AR* model of order p at j-th measured

acceleration signal, or AR (p), for the time series can be written as

$$A_j(q)x_j(k) = e_j(k) \tag{4}$$

$$A_j(q) = 1 + a_{1j}q^{-1} + a_{2j}q^{-2} + \cdots + a_{pj}q^{-p} \tag{5}$$

where $x_j(k)(j = 1, 2, \cdots, m, k = 1, 2, \cdots, n)$ are the current and previous values of the time series and $e_j(k)$ is *AR* model residual error. The *AR* coefficients $a_{1j}, a_{2j}, \cdots, a_{pj}$ can be evaluated using a variety of methods. Here, the coefficients were calculated using the Yule-Walker equations (Box and Jenkins 1976). For the structural reference (health) state, the corresponding *AR* model can be made, the model parameter $A_j^{ref}(q)$ and residual error $e_j^{ref}(k)$ can be obtained. Similarly, for any unknown structural test sample $y_j(k)$, its residual error is,

$$e_j^{test}(k) = A_j^{test}(q)y_j(k) \tag{6}$$

If the residual error is assumed as a Gaussian normal distribution with a zero mean, the traditional damage-sensitive index (DI) is defined as the standard deviation (STD) ratio of the unknown test state to the reference one as follows (Sohn and Farrar 2001),

$$\gamma^{std}(e_j) = \sigma(e_j^{test}) / \sigma(e_j^{ref}) \tag{7}$$

When the test samples come from the structural health state, AR model can effective predict the sample, therefore the variance of the residual error is close to one of the reference sample, the STD ratio in Eq. (7) is approximately equal to one. When the test samples come from the structural damage state, the residual error will be increased, the STD ratio will larger than one, therefore, the STD ratio can be used to determine if the structures is damaged or not.

2.3 Order of AR model

The order of the *AR* model is an unknown value. A high-order model may perfectly match the data, but will not generalize to other data sets. On the other hand, a low-order model will not necessarily capture the underlying physical system response. In order to find out the optimum model order, several techniques are used in this study, such as Akaike's information criterion (*AIC*), partial autocorrelation function (*PAF*), final prediction error (*FPE*) etc. Finally, the *AIC* is selected in this study, which is used to assess the generalization performance of linear models. In a simple way, this technique returns a value that is the sum of two terms as follows

$$AIC = -2L_m + 2m \tag{8}$$

Where L_m is the maximized log-likelihood of the residual error, and *m* is the number of adjustable parameters in the model. It assumes a tradeoff between the fit of the model and the model's complexity. The first term is related to how well the model fits the data, i.e., if the model is too simple, the residual errors increase. On the other hand, the second term is a penalty factor related to the complexity of the model, which increases as the number of additional parameters grows (Box and Jenkins 1976).

2.4 Nonlinear damage-sensitive index

It should be noted that AR model is a kind of linear model and many classical statistical tests depend on the assumption of normality. This approach is based on the

assumption that damage will introduce either linear deviation from the baseline condition or nonlinear effects in the signal and, therefore, the linear model developed with the baseline data will no longer accurately predict the response of the damaged system.

In order to establish the underlying distribution of the data, some higher statistical moments are used to estimate the probability density function (PDF) of the measured signals without normal distribution. Moreover, it is expected that the damage can introduce significant changes in the acceleration-time-history PDFs and, as a consequence, the third and fourth statistical moments and PDFs are introduced as damage-sensitive features in this study.

The third statistical moment is a measure of the asymmetry of the PDF. The normalized third statistical moment is called the skewness and is defined as

$$skewness(e_j) = E[e_j - m(e_j)]^3 / \sigma(e_j)^3 \tag{9}$$

where a positive skewness represents that the right tail is longer and that the area of the distribution is concentrated below the mean. On the other hand, a negative skewness means that the left tail is longer and that the area of the distribution is concentrated above the mean. The skewness of a standard normal distribution is zero.

The fourth statistical moment is a measure of the relative amount of data located in the tails of a probability distribution. The kurtosis is the normalized fourth statistical moment and is defined as

$$kurtosis(e_j) = E[e_j - m(e_j)]^4 / \sigma(e_j)^4 \tag{10}$$

where a kurtosis greater than three indicates a “peaked” distribution that has longer tails than a standard normal distribution. This means that there are more cases far from the mean. Kurtosis less than three indicates a “flat” distribution with shorter tails than a standard normal distribution. This property implies that fewer realizations of the random variable occur in the tails than would be expected in a normal distribution. The kurtosis of a standard normal distribution is three.

Similar to Eq. (7), two damage-sensitive indexes are defined as the Skewness and Kurtosis ratio of structural unknown test state to its reference state as follows,

$$\gamma^{skew}(e_j) = \left| skewness(e_j^{test}) / skewness(e_j^{ref}) \right| \tag{11}$$

$$\gamma^{kur}(e_j) = kurtosis(e_j^{test}) / kurtosis(e_j^{ref}) \tag{12}$$

When the structure is in a health state, the skewness of the AR model residual error is close to zero, its kurtosis approaches to three. When the structure is damaged, the skewness will be positive or negative, the kurtosis will increase. When the test and reference samples come both from same state, the skewness and kurtosis will be identical and equal to one, or else they will be more or less than one, which can be used to detect the damage of structures.

2.5 Integrated damage-sensitive indexes

The damage-sensitive index (DI) in Eq. (7) is a linear traditional index, Eqs. (11-12) are just partial DI indexes. In order to integrate their function at the same time, six DIs are defines as follows in terms of arithmetic and geometric average meanings,

$$DI_1 = (\gamma^{std} + \gamma^{skew}) / 2 \tag{13}$$

$$DI_2 = (\gamma^{std} + \gamma^{kur})/2 \tag{14}$$

$$DI_3 = (\gamma^{std} + \gamma^{skew} + \gamma^{kur})/3 \tag{15}$$

$$DI_4 = \sqrt{\gamma^{std} \times \gamma^{skew}} \tag{16}$$

$$DI_5 = \sqrt{\gamma^{std} \times \gamma^{kur}} \tag{17}$$

$$DI_6 = \sqrt[3]{\gamma^{std} \times \gamma^{skew} \times \gamma^{kur}} \tag{18}$$

2.6 Structural damage detection (SDD)

In the previous section, damage indexes have been defined, but it is difficult to choose a threshold values that characterize damage. In order to perform the damage detection, fuzzy c-means clustering (*FCM*) algorithm, which was first presented by Bezdek (1981), and recently applied to SHM problems by da Silva et al. (2008), is employed to clarify the features, and supply a fuzzy decision by using the membership of damage index in a cluster. This algorithm is an unsupervised classification algorithm which uses a certain objective function, described in Eq. (19), for iteratively determining the local minima.

$$\min J(C,m) = \sum_{i=1}^{C}\sum_{j=1}^{N} u_{ij}^{m} d_{ij}^{2} \tag{19}$$

$$center_i = \sum_{j=1}^{N} u_{ij}^{m} x_j \Big/ \sum_{j=1}^{N} u_{ij}^{m} \tag{20}$$

$$d_{ij}^{2} = (x_j - center_i)^{T}(x_j - center_i) \tag{21}$$

$$u_{ij} = (d_{ij})^{\frac{-2}{m-1}} \Big/ \sum_{k=1}^{C} (d_{kj})^{\frac{-2}{m-1}} \tag{22}$$

where C is the total number of clusters and N is the total number of objects in calibration. u_{ij} is the membership function associated with the j-th object of the i-th cluster, which is updated by using Eq. (22) in each iteration step. The exponent m is a measurement of fuzzy partition. $center_i$ is the centroid of the i-th cluster, x_j is j-th object of data set to be clustered, which is set to be any of DSIs here, d_{ij} denotes the distance between j-th object and the centroid of the i-th cluster, here, Euclidean distance is used as Eq. (21) (Matlab 2010).

3. EXPERIMENTAL VERIFICATION

In order to assess the performance of the integrated SDD method proposed in this study, some experimental data from the three-story building structure are adopted here, which is downloaded from the web site of the Los Alamos National Laboratory (LANL), USA (Figueiredo et al. 2009). The three-story building structure as shown in Fig. 1 is used as a damage detection test bed, in which some detailed layout of the mass added at the base and nonlinearity source are shown in Fig. 2.

3.1 Structural damage scenarios

The nonlinear damage was introduced through nonlinearities resulting from impacts with a bumper. When the structure is excited at the base, the suspended column hits

the bumper. The level of nonlinearity depends on the amplitude of oscillation and the gap between the column and the bumper. The operational and environmental variety was simulated by adding mass and reducing stiffness at several different locations. Force and acceleration time series samples recorded for a variety of different structural state conditions were collected as shown in Table 1 together with information that describes the different states. Each state includes 10 observed cases, each case records 8192 consecutive data samples. For example, State#13-6-Test indicates the sixth observed data with case no of 126 in Table 1 for State #13 under unknown test condition. Therefore, there are 170 cases for 17 states in total, as listed in Table 1.

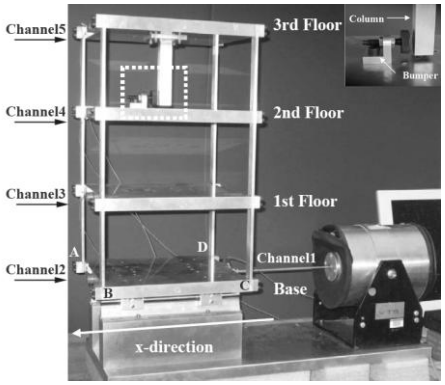

Fig. 1 Three-story building model

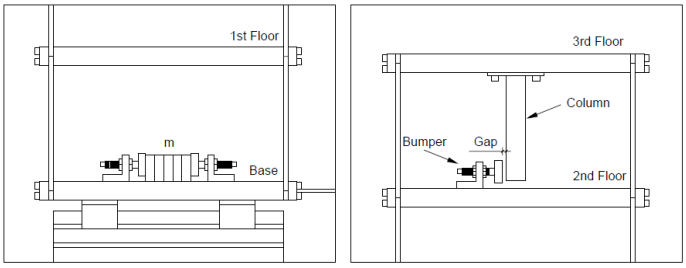

(a) Mass, m, added at the base (b) Nonlinearity source

Fig. 2 Added mass and nonlinearity source

Table 1 Data labels of structural state conditions

Group	State	Case	State condition	Description
1	State #1	1-10	Undamaged	Baseline condition
2	State #2	11-20	Undamaged	Mass = 1.2 kg at the base
	State #3	21-30	Undamaged	Mass = 1.2 kg on the 1st floor
	State #4	31-40	Undamaged	87.5% stiffness reduction in column 1BD
	State #5	41-50	Undamaged	87.5% stiffness reduction in column 1AD and 1BD
	State #6	51-60	Undamaged	87.5% stiffness reduction in column 2BD
	State #7	61-70	Undamaged	87.5% stiffness reduction in column 2AD and 2BD
	State #8	71-80	Undamaged	87.5% stiffness reduction in column 3BD
	State #9	81-90	Undamaged	87.5% stiffness reduction in column 3AD and 3BD
3	State #10	91-100	Damaged	Gap = 0.20 mm
	State #11	101-110	Damaged	Gap = 0.15 mm
	State #12	111-120	Damaged	Gap = 0.13 mm
	State #13	121-130	Damaged	Gap = 0.10 mm
	State #14	131-140	Damaged	Gap = 0.05 mm
4	State #15	141-150	Damaged	Gap = 0.20 mm and mass = 1.2 kg at the base
	State #16	151-160	Damaged	Gap = 0.20 mm and mass = 1.2 kg on the 1st floor
	State #17	161-170	Damaged	Gap = 0.10 mm and mass = 1.2 kg on the 1st floor

From Table 1, it can be found that the structural state conditions can be categorized into four main groups. The first group (State #1) is the baseline condition. The second group includes the states (States #2-#9) when the mass or stiffness of the structure are changed. Real-world structures have operational and environmental variability, which create difficulties in detecting and identifying structural damage. Such variability often manifests itself in linear changes in the stiffness or mass of a structure. In order to simulate such operational and environmental condition changes, tests are performed with different mass and stiffness conditions (States #2-#9). For example, the state condition labeled "State #4" described in Table 1 means that there is a 87.5% stiffness reduction in the columns located between the base and 1st floor at the intersection of plane B and D as illustrated in Fig. 2(b) by (Figueiredo et al. 2009, Chen and Yu 2013) (abbreviated as 1BD, other abbreviations can be identified in the similar way). The stiffness reduction consists of replacing the corresponded column by another one with half the cross section thickness in the direction of shaking. The third group includes damaged state conditions (States #10-#14) simulated through the introduction of nonlinearities into the structure using a bumper and a suspended column, with different gaps between them. Finally, the fourth group includes the state conditions (States #15-#17) with nonlinear damage in addition to mass and stiffness changes used to simulate operational and environmental condition changes.

3.2 Effects of environmental conditions and structural damage

The dynamic characteristics of structures are easily affected by either structural damage or the operational environment conditions. How to determine whether it is due to the former or the latter, it is not easy. Sometimes the change in dynamic characteristics due to the latter is more significant than one by the former. Using the measured excitation force and acceleration responses, the frequency response function (FRF) can be obtained under the different conditions, as shown in Fig. 3. It can be seen from Fig. 3(a) that the structural frequencies have been shifted due to adding mass (State #3) or stiffness reduction (State #9) as compared with the FRF curve of baseline health condition of structure (State #1) at Channel 5 although the structure is all in undamaged conditions. If the structural damage conditions (States #14 & 17) are compared with the baseline health one, Fig. 3(b) shows that the second frequency of structure will be increased under the nonlinear damage of structure (State #14). Further, the third frequency of structure will be decreased if both the environmental condition and nonlinear damage are considered simultaneously (State #17). Therefore, it is very difficult to estimate the structural damage if the frequencies of structures are considered only.

3.3 Traditional damage-sensitive indexes

Fig. 4 shows the effects of AR model orders on the AIC of measured accelerations in baseline state (State #1). It can be seen that the changes in AIC curves are very small when the AR order is equal to or higher than 50, therefore, AR (50) is determined for prediction of the test samples in the following section. Fig. 5 compared the time histories of the measured acceleration responses with the fitted ones by using the AR (50) model. It can be found that the fitted ratio are reached to 68.3%, 85.8%, 92.59% and 90.08% for the data measured at Channels 2, 3, 4 and 5 respectively.

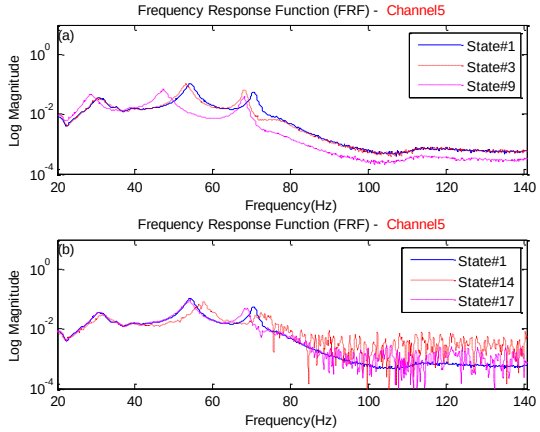

Fig. 3 Comparison on FRF curves

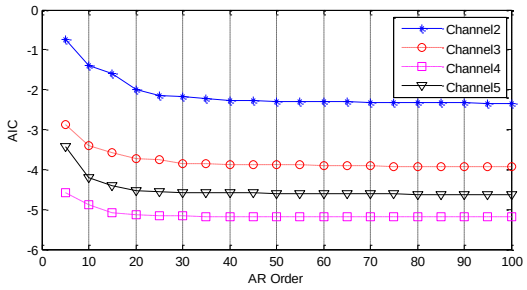

Fig. 4 Determination of AR model order

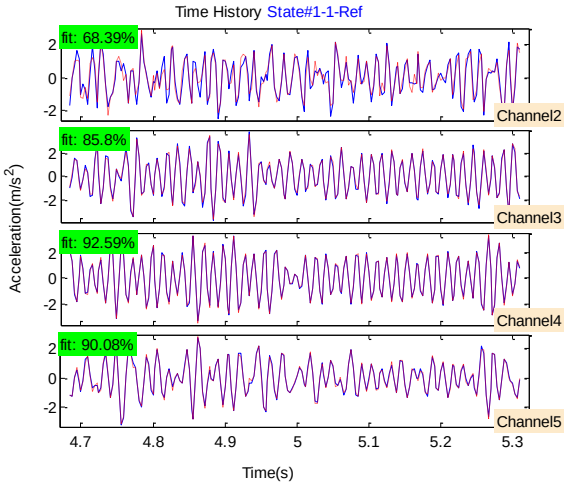

Fig. 5 Meansured and fitted data

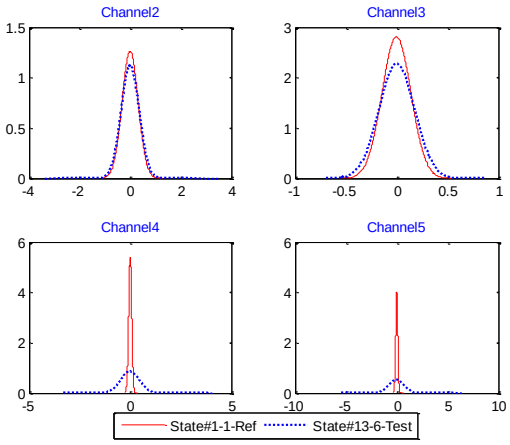

Fig. 6 PDFs of AR residuals

Moreover, the residual errors are calculated, the estimated probability density functions (PDFs) of residual errors are compared in Fig. 6. which are corresponding to State #1 in red solid line and State #13 in blue dotted line respectively. As listed in Table 1, the State #1 indicates one undamaged state of structure, but the State #13 represents a damaged one, in which the gap between the column and the bumper is set to be 0.1 mm. It can be seen that the estimated PDFs of residual errors has changed obviously after the damage occurs in the State #13 condition, particular for the Channels 4 and 5 near the gap. Therefore, the changes in the PDFs of residual errors can be used to identify the structural damage. The standard deviation (STD) ratios of the unknown test state to the reference one, as defined in Eq. (7), are shown in Fig. 7 for all 170 cases under 17 states in total as listed in Table 1. The damaged and undamaged states can be easily identified.

3.4 Extraction of integrated damage-sensitive indexes

Normal probability testing of AR residual errors in State#13-6 is shown in Fig. 8. It can be found that the unknown test State #13-6 is a damaged state because the AR

residual errors are deviate from the normal distribution, particular for ones in Channels 4 and 5. It will not completely reflect the statistical distribution if the standard deviation (STD) of AR residual errors are used only. The histogram of AR residual errors in State #13-6 is compared with the normal fitting PSD curves in solid red line in Fig. 9, which indicates that the distribution of residual errors is obviously different from the normal fitting PSD curves, particularly at channels 4 and 5, the kurtosis of AR residual errors are greatly higher than ones of the normal fitting PSD.

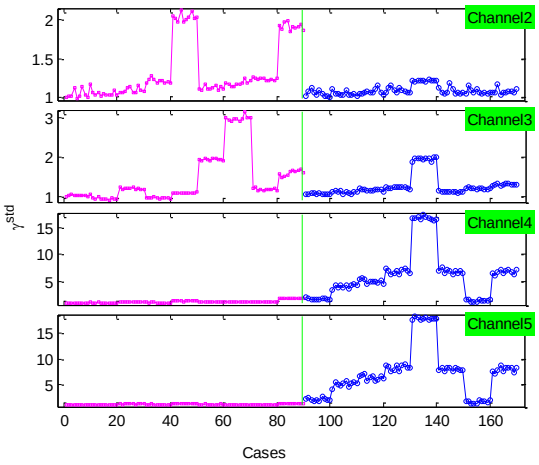

Fig. 7 STD ratios for all 170 cases

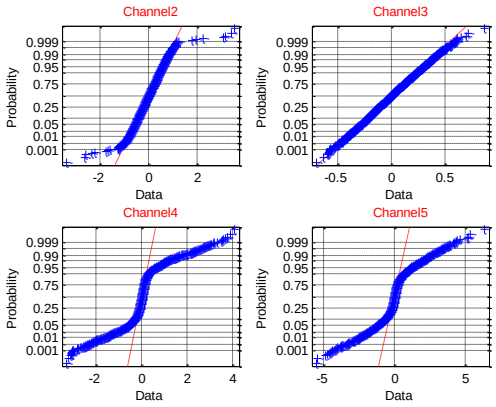

Fig. 8 Normal probability testing

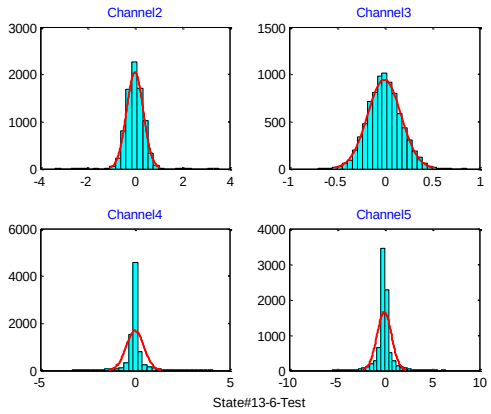

Fig. 9 Histogram with normal fitting

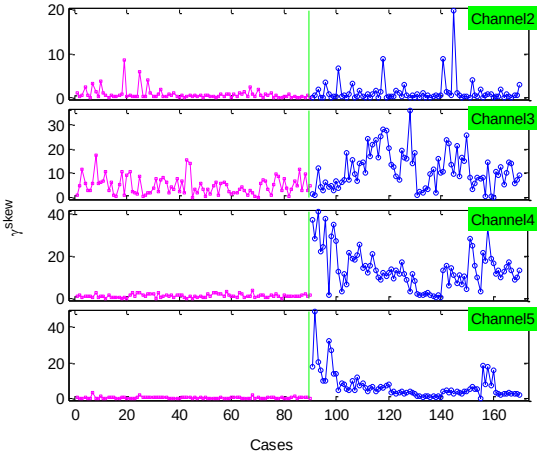

Fig. 10 Skewness ratios for cases

For all 170 cases under 17 test states in total as listed in Table 1, the skewness and kurtosis ratios of structural unknown test state to its reference state, as defined in Eqs. (11) and (12), are calculated and shown in Figs. 10 and 11 respectively. If they are compared with ones in Fig. 7, it can be found that after the structure is damaged, the states with lower STD ratios at channels 4 and 5 in Fig. 7, i.e.. states #10 and #16, correspond to ones with higher skewness ratios and kurtosis ratios at channels 4 and 5 in Figs. 10 and 11. This shows that the skewness and kurtosis ratios are the complementary to the STD ratio.

Further, six integrated damage-sensitive indexes are calculated and shown in Fig. 12. In comparison to the STD ratios in Fig. 7, it can be seen that the distribution of damaged indexes are more reasonable, the damaged and undamaged states of the structure can be easily identified.

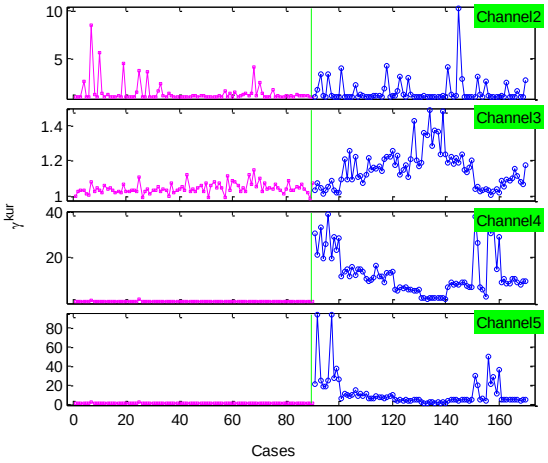

Fig. 11 Kertosis ratios for cases

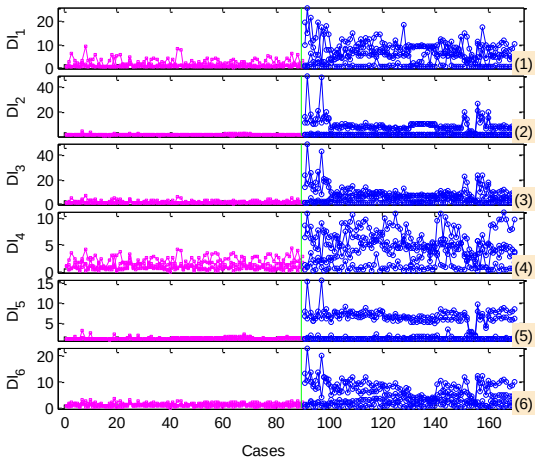

Fig. 12 Integrated damaged-sensitive indexes

3.5 Structural damage detection

In order to perform the SDD, the fuzzy c-means clustering (*FCM*) algorithm is employed to clarify the damage-sensitive features and used to supply a fuzzy decision by using the membership of damage index in a cluster as defined in Eq. (19). Here, the computation parameters C=2 and m=2 respectively. The analytical results of membership for the traditional STD ratio is shown in Fig. 13. It can be found that there are no damage in both states #10 and #16. In fact, the both SDD results are not correct because both states #10 and #16 are in damaged states. In comparison to other states, there are the largest gap between the column and the bumper, i.e. 0.2 mm, in both states #10 and #16. There are fewer opportunity to hit each other when the structure is excited, so the nonlinear damage severity is lower as well. However, the SDD result is correct in state #15 although the gap and the added mass are the same as ones in states #16. Only one difference between them is the different locations of added mass. It is at the base in state #15 but on the first floor in state #16. This affects the nonlinear interaction between the column and the bumper when the structure is excited at the base. It is also shown that the traditional STD ratio is easily affected by the environmental variability.

All the membership results from six integrated DIs are listed in Table 2, in which, abbreviated capital character 'FP', i.e. false positive, represents that the healthy state of structure is deemed as the damage state. While 'FN', i.e. false negative, means that the damage state of structure is deemed as the healthy state. Moreover, sign 'xx/yy' indicates that there are xx misdiagnoses out of yy data sample cases. The criterion of diagnosis decision is accepted as the follows: the structure is deemed as a the healthy state if the membership value is lower than 0.5, otherwise, it is in a damage state.

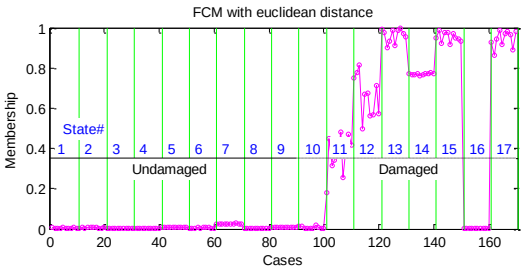

Fig. 13 Membership due to STD ratio

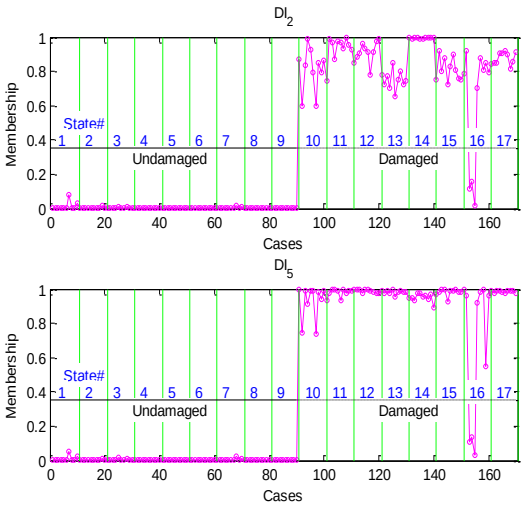

Fig. 14 Membership due to DI_2 and DI_5

Table 2 Membership results for integrated damage-sensitive indexes

State	γ^{std}	DI_1	DI_2	DI_3	DI_4	DI_5	DI_6
FP	0/89	0/89	0/89	0/89	0/89	0/89	0/89
FN	**31/80**	**3/80**	**3/80**	**2/80**	**5/80**	**3/80**	**13/80**
1	0/9	0/9	0/9	0/9	0/9	0/9	0/9
2	0/10	0/10	0/10	0/10	0/10	0/10	0/10
3	0/10	0/10	0/10	0/10	0/10	0/10	0/10
4	0/10	0/10	0/10	0/10	0/10	0/10	0/10
5	0/10	0/10	0/10	0/10	0/10	0/10	0/10
6	0/10	0/10	0/10	0/10	0/10	0/10	0/10
7	0/10	0/10	0/10	0/10	0/10	0/10	0/10
8	0/10	0/10	0/10	0/10	0/10	0/10	0/10
9	0/10	0/10	0/10	0/10	0/10	0/10	0/10
10	**10/10**	0/10	0/10	0/10	0/10	0/10	0/10
11	**10/10**	**1/10**	0/10	0/10	0/10	0/10	0/10
12	**1/10**	0/10	0/10	0/10	0/10	0/10	0/10
13	0/10	0/10	0/10	0/10	0/10	0/10	0/10
14	0/10	0/10	0/10	0/10	**2/10**	0/10	**10/10**
15	0/10	0/10	0/10	0/10	0/10	0/10	0/10
16	**10/10**	**2/10**	**3/10**	**2/10**	**3/10**	**3/10**	**3/10**
17	0/10	0/10	0/10	0/10	0/10	0/10	0/10

It can be seen from Table 2 that all membership results from six DIs, i.e. from DI_1 through DI_6, are better than ones due to the traditional STD ratio (γ^{std}). The best result is from the DI_3 because there are only two misdiagnosis out of 169 data sample cases. DI_3 is the arithmetic average value of STD, skewness and kurtosis ratios of AR residual errors. Therefore, the skewness and kurtosis indexes can provide a benefic complement to the traditional STD ratios. This also indicates that the complementary among STD, skewness and kurtosis ratios has been verified.

Moreover, it can be also found that the results from DI_2 and DI_5, both due to STD and kurtosis ratios in the arithmetic or geometric way, are better than ones due to both DI_1 and DI_4. The membership results due to DI_2 and DI_5 are shown in Fig. 14. Further, the DI_5 results are a little bit better than the DI_2 result because the distribution of DI_5 membership results are closer to the damage membership value of 100% as a whole when the structure is under all the nonlinear damaged states #10-#17, which indicates that all the nonlinear damaged states can be effectively identified.

4. CONCLUSIONS

In this study, an integrated method is proposed for structural nonlinear damage detection based on time series analysis, the higher statistical moments of structural responses and the fuzzy c-means (FCM) clustering techniques. Six comprehensive damage-sensitive indexes (DIs) are developed in the arithmetic and geometric manner of the higher statistical moments, and are classified by using the FCM clustering method to achieve nonlinear damage detection. Some experimental data downloaded from the web site of the Los Alamos National Laboratory (LANL) USA on a three-story building structure are adopted to assess the effectiveness and robustness of the new nonlinear structural damage detection (SDD) method proposed in this study. The illustrated results show that: (1) The proposed integrated method is an effective tool for structural nonlinear damage detection, the damaged and undamaged states of the structure can be easily identified based on the newly proposed method. (2) The traditional standard deviation (STD) ratio of the residual errors is easily affected by the environmental variability. The skewness and kurtosis indexes can provide a benefic complement to the traditional STD ratio. (3) All membership results from six integrated DIs, i.e. from DI_1 through DI_6, are better than ones due to the traditional STD ratio. The distribution of six integrated DIs are more reasonable. The best result is from the DI_3 in the arithmetic average value of STD, skewness and kurtosis ratios of AR residual errors. DI_2 and DI_5, both due to STD and kurtosis ratios in the arithmetic or geometric way, are better than ones due to both DI_1 and DI_4. (4) Although the proposed integrated methodology showed great success for the examples under investigation, the authors also acknowledged that the methodology should be verified with more laboratory experiments using different types of structures in the field of structural engineering.

ACKNOWLEDGEMENTS

The project is jointly supported by the National Natural Science Foundation of China (50978123, 51278226 and11032005). The authors would like to acknowledge the Los Alamos National Laboratory (LANL) USA for freely downloading the experimental data of the three-story building structure used in this study.

REFERENCES

Bezdek, J.C. (1981), “Pattern recognition with fuzzy objective function algorithm”, Plenum Press, NY.

Box, G. and Jenkins, G. (1976), "Time series analysis: forecasting and control", Prentice Hall, Englewood Cliffs, New Jersey.

Carden, E.P. and Brownjohn, J.M. (2008), "ARMA modelled time-series classification for structural health monitoring of civil infrastructure", *Mech. Syst. Sig. Process.,* **22** (2), 295-314.

Carden, E.P. and Fanning, F. (2004), "Vibration based condition monitoring: a review", Structural Health Monitoring, **3**(4), 355-377.

Chen, L.J. and Yu, L. (2013), "Structural nonlinear damage identification algorithm based on time series ARMA/GARCH model", *Advances in Structural Engineering*, **16**(9): 1597-1609.

da Silva, S., Dias Júnior, M., Lopes Junior, V. and Brennan, M.J. (2008), "Structural damage detection by fuzzy clustering", *Mech. Syst. Sig. Process.,* 22, 1636-1649.

Doebling, S.W., Farrar, C.R. and Prime, M.B. (1998), "A summary review of the vibration-based damage identification methods", *Shock Vib. Dig.*, 30(2), 91-105.

Figueiredo, E., Park, G., Figueiras, J. Farrar, C. R. and Worden, K. (2009), "Structural health monitoring algorithm comparisons using standard data sets", Los Alamos National Laboratory Report, LA-14393.

Fugate, M.L., Sohn, H. and Farrar, C. R. (2001), "Vibration-based damage detection using statistical process control", *Mech. Syst. Sig. Process.,* **15**(4), 707-721.

Gul, M. and Catbas, F.N. (2009), "Statistical pattern recognition for structural health monitoring using time series modeling: theory and experimental verifications", *Mech. Syst. Sig. Process.,* **23** (7), 2192-2204.

Gul, M. and Catbas, F.N. (2011), "Structural health monitoring and damage assessment using a novel time series analysis methodology with sensor clustering", *J. Sound and Vib.*, **330**(6), 1196-1210.

Lu, Y. and Gao, F. (2005), "A novel time-domain auto-regressive model for structural damage diagnosis", *J. Sound and Vib.*, **283**(3-5), 1031-1049.

MATLAB (2010), Statistics Toolbox, User's Guide, http://www.mathworks.com, The MathWorks, Inc.

Mattson, S. and Pandit, S. (2006), "Statistical moments of autoregressive model residuals for damage localization", *Mech. Syst. Sig. Process.*, **20**, 627-645.

Nair, K.K., Kiremidjian, A.S. and Law, K.H. (2006), "Time series-based damage detection and localization algorithm with application to the ASCE benchmark structure", *J. Sound and Vib.*, **291**(1-2), 349-368.

Omenzetter, P. and Brownjohn, J.M. (2006), "Application of time series analysis for bridge monitoring", *Smart Mater. Struct.*, **15**, 129-138.

Sohn, H. and Farrar, C. R. (2001), "Damage diagnosis using time series analysis of vibration signals", *Smart Mater. Struct.*, **10**, 1-6.

Sohn, H., Farrar, C.R., Hemez, F.M., Shunk, D.D., Stinemates, D.W. and Nadler, B.R. (2004), "A review of structural health monitoring literature: 1996-2001", Los Alamos National Laboratory Report.

Worden, K., Farrar, C. R., Manson, G. and Park, G. (2007), "The fundamental axioms of structural health nonitoring", *Proceedings of the Royal Society*, **463**, 1639-1664.

Yan, Y.J., Cheng, L., Wu, Z.Y. and Yam, L.H. (2007), "Development in vibration-based structural damage detection technique", *Mech. Syst. Sig. Process.*, **21**, 2198-2211.

Yao, R. and Pakzad, S.N. (2014), “Damage and noise sensitivity evaluation of autoregressive features extracted from structure vibration”, *Smart Mater. Struct.* **23**, 025007.

Yao, R. and Pakzad, S.N. (2012). “Autoregressive statistical pattern recognition algorithms for damage detection in civil structures”, *Mech. Syst. Sig. Process.*, **31**, 355-368.

Yu, L., Zhu, J.H. and Yu, L.L. (2013), “Structural damage detection in a truss bridge model using fuzzy clustering and measured FRF data reduced by principal component projection”, *Advances in Structural Engineering*, **16**(1): 207-217.

Zhang, Q.W. (2007), “Statistical damage identification for bridges using ambient vibration data”, Computers and Structures, **85**, 476-485.

Zhou, L.R., Yan, G.R., Wang, L. and Ou, J.P. (2013), “Review of benchmark studies and guidelines for structural health monitoring”, *Advances in Structural Engineering*, **16**(7),1187-1206.

Zugasti, E., Gómez González, A., Anduaga, J., Arregui, M. A. and Martínez, F. (2012), “NullSpace and AutoRegressive damage detection: a comparative study”, *Smart Mater. Struct.* 21, 085010.